Proceedings of ASME Turbo Expo 2024
Turbomachinery Technical Conference and Exposition
GT2024
June 24-28, 2024, ExCeL
London, England, United Kingdom

GT2024-125893

SUPERSONIC CONVERGENT-DIVERGENT VANED NOZZLES DESIGN ALGORITHM AND RESPECTIVE DISCHARGE COEFFICIENT MODEL

Leonid Moroz
SoftInWay Inc.
Burlington, MA

Maksym Burlaka
SoftInWay Inc.
Burlington, MA

Boris Frolov
SoftInWay Switzerland
Zug, Switzerland

Tetiana Dyzenko
SoftInWay Switzerland
Zug, Switzerland

ABSTRACT

To continue the series of already published articles on supersonic drilled nozzles [GT2022-83387, GT2023-101760], this publication is devoted to another type of supersonic nozzles, which are formed by vanes providing an annular row of convergent-divergent supersonic channels. This type of supersonic vaned nozzles, as well as the drilled nozzles, are used in numerous high-loaded turbine applications. Published data on this type of nozzles and turbine stages with them have very limited information on both the design methodology and calculation methods and thus do not allow these data to be systematized and implemented into the turbine design and calculation tool. The work carried out in this direction includes all the algorithms and models required for the supersonic vaned nozzle design and calculations: (1) The design algorithm of a highly efficient supersonic vaned nozzle, (2) the discharge coefficient model, (3) loss model, (4) flow angle deviation model. In this article, we focus on design model (1) and discharge coefficient (2) items. A list of geometric parameters that uniquely determine the 3D geometry of the nozzle channel that is used in the design algorithm is discussed. The approaches to building convergent and divergent parts of the supersonic nozzle are elaborated. Besides, the model of the discharge coefficient through the critical section of the nozzle is described in detail. The developed discharge coefficient model demonstrated a maximal deviation of 0.6% and an average of 0.18% from CFD results in a wide range of configurations of the nozzle channel

Keywords*: Supersonic Turbine, Vaned nozzles, Convergent-Divergent Nozzles, Turbine Performance, Aerodynamic Losses, CFD, Turbine Design, Turbine Analysis.*

NOMENCLATURE

alpha	[degree]	divergent part axis angle
a_{exit}	[m]	outlet channel width at a planar profile
a_{cr}	[m]	critical throat at a planar profile
A_{exit}	[m^2]	3D area at nozzle exit $A_{exit}= a_{exit} \cdot H$
A_{cr}	[m^2]	3D critical throat area $A_{cr}= a_{cr} \cdot H$
A_{in}	[m]	distance between LE circles
A_{in_min}	[m]	minimal distance between LE circles
b	[m]	chord (for traditional turbine profiles)
C_{cr}	[m/s]	isentropic critical velocity.
C_d	[-]	discharge coefficient
C_{d_base}	[-]	base discharge coefficient
C_{d_slip}	[-]	discharge coefficient for free slip walls
C_{max}	[m]	maximum profile width.
conv	[-]	convergence factor
D	[m]	mean diameter
G	[kg/s]	nozzle ring mass flow rate
G_1	[kg/s]	nozzle mass flow rate per 1 channel
G_{ideal}	[kg/s]	ideal mass flow rate (MFR), calculated via isentropic parameters at critical throat.
H	[m]	nozzle height
H_{rel}	[-]	relative height, $H_{rel}=H/ a_{cr}$
H_{ax}	[m]	axial distance between the leading edge arc center and the critical throat center

H_{ax_rel}	[-]	relative axial distance, $H_{ax\_rel} = H_{ax} / a_{cr}$
H_{tan}	[m]	tangential distance between the leading edge suction side arc center and the critical throat center
H_{tan_rel}	[-]	relative tangential distance, $H_{tan\_rel} = H_{tan} / a_{cr}$
I_0^*	[J/kg]	inlet total enthalpy
K_{Roug}	[-]	discharge coefficient correction factor on the channel walls roughness
K_{H_rel}	[-]	discharge coefficient correction factor on the relative nozzle height
k	[-]	isentropic exponent $k=Cp/Cv$
L	[m]	divergent channel length
L_d	[-]	divergent channel length factor
L_{ideal}	[m]	ideal divergent part length (built by MOC)
M_t	[-]	isentropic Mach number
P_{cr}	[Pa]	critical static pressure
P_0^*	[Pa]	inlet total pressure
P_s	[Pa]	static pressure at nozzle exit
phi_{ss}	[degree]	leading edge arc angle at suction side
phi_{ps}	[degree]	leading edge arc angle at pressure side
pa	[-]	partial admission ratio $pa=t \cdot z/(\pi \cdot D)$
PR	[-]	nozzle design pressure ratio
R	[J/(kg K)]	gas constant
r_1	[m]	leading edge (LE) radius
r_{1_rel}	[-]	relative leading edge (LE) radius, $r_{1\_rel} = r_1 / a_{cr}$
r_2	[m]	trailing edge (TE) radius
R_c	[m]	wall curvature radius
R_t	[m]	critical throat radius $R_t=a_{cr}/2$
Re	[-]	Reynolds number by critical throat, critical velocity and viscosity by critical parameters
Re_d	[-]	Reynolds number by the hydraulic diameter of the critical throat area, critical velocity and viscosity by critical parameters.
t	[m]	pitch at mean diameter
T_0^*	[K]	inlet total temperature
XPR	[-]	expansion ratio
z	[-]	number of opened nozzle channels
ΔC_{d_Re}	[-]	discharge coefficient correction function on Reynolds number
ρ_0^*	[kg/m^3]	inlet density by total parameters
ρ_{cr}	[kg/m^3]	isentropic critical density

Subscripts

ss	suction side
ps	pressure side
cr	critical

Acronyms

CDV	supersonic convergent-divergent vaned nozzle
MOC	method of characteristics
MFR	mass flow rate

1. INTRODUCTION

In many turbine applications, the general trend towards reduced weight, cost, and design simplification is leading to the use of high-load turbine stages with transonic and supersonic flow. At the same time, the performance of supersonic stages depends both on the characteristics of nozzles and rotor blades and on their interaction in various operation modes. The supersonic flow in the nozzle and rotor blade channels is complex and must be taken into account in both design and performance analysis.

A large number of publications, both experimental and computational, are devoted to the tasks of designing and evaluating the characteristics of supersonic stages, considering various aspects of design and parameter calculation [1-12].

To achieve supersonic velocities, the channel should have a convergent-divergent configuration, first developed by Gustaf de Laval. The relationship between the cross-sectional area and the Mach number is given by the following equation [13-14] for the isentropic process of perfect gas:

$$\frac{dA}{A} = \frac{M_t^2 - 1}{M_t \cdot (1 + \frac{k-1}{2} M_t^2)} dM_t, \quad (1)$$

The factor $M_t^2 - 1$ determines different relationships between cross-section area and velocity in the channel for two cases $Mt<1$ and $Mt>1$. In the case of $Mt>1$, the Mach number increases with the cross-section area increase and vice versa. The special case is when $M=1$ which requires that $dA=0$ at minimum cross-section area which is referred to as "critical throat".

The ratio of the outlet area to the area in the critical throat of the channel also referred to as an expansion ratio XPR, could be defined via Mach number for the isentropic process of perfect gas.

$$XPR = \frac{A_{exit}}{A_{cr}} = \left(\frac{2}{k+1}\right)^{\frac{k+1}{2(k-1)}} \frac{\left(1 + \frac{k-1}{2} M_t^2\right)^{\frac{k+1}{2(k-1)}}}{M_t} \quad (2)$$

Structurally, turbine nozzles of this type can be made by technologically different methods - historically, the first and the simplest manufacturing option is a drilled-type nozzle with an expanding part reamed on a cone. Article [11] presents data on the optimization of this type of nozzle and the results of the stages efficiency calculation vs the authors' testing data. With all the advantages associated with the technological simplicity of manufacture, such nozzles have some an inherent peculiarity of the oval structure of the jet, which leads to incomplete fill of the section at the outlet of the nozzle and at the inlet to the rotor blade and hence higher losses at certain conditions.

The supersonic channels formed by vanes and creating an annular row of convergent-divergent channels, similar to the traditional type of subsonic turbine nozzles do not have this drawback. In such types of channels, the supersonic flow at the nozzle exit fills the entire annular section at the inlet to the rotor blades.

A complete model of such a supersonic vaned turbine nozzle with a symmetrical divergent part was developed in the course of this work and implemented into the turbine design tool. It is based on a set of independent geometric parameters, which together with inlet/outlet thermodynamic parameters and functions of the working fluid, uniquely determine the 3D geometry of the nozzle. The same set of parameters is directly related to the models of discharge coefficient, losses, and deviation angle. Using this set of information, it is possible to create a highly efficient supersonic nozzle and at the same time satisfy the structural characteristics and design constraints of the turbine stage.

In this article, we focus on two aspects of supersonic nozzle development:

- Design methodology - description of the parametric model design data and its calculation for given thermodynamic inlet/outlet parameters.
- Discharge coefficient model development and calculation for the designed nozzle.

1.1 Nozzle Design Methodology.

A wide variety of profiling methods are available for vaned turbine nozzles [15-25]. The traditional approach to turbine nozzles profiling is based on the use of chord b as the basic element of the profile and experimentally tested relationships between the main geometric parameters, such as relative pitch to chord ratio t/b, relative height b/H, relative profile thickness C_{max}/b to select other required parameters, such as stagger angle, leading-edge radius, etc. In this approach, profiling of the channel walls is performed using curves of the second or high order [15, 16]. Thus, Figure 1 shows several variants of traditional nozzle blade channels from the M. E. Deich atlas [24]. The atlas presents a series of profiles covering the ranges of Mach numbers from subsonic M=<0.6-0.9 (Figure 1a) to transonic M=<0.9-1.2 (Figure 1b and 1c) and supersonic with Mach numbers M=< 1.2-1.5 (Figure 1d). This group of nozzles is characterized by a traditional convergent shape of the channel from the inlet to the throat. The suction side section after the throat in the region of the uncovered outlet channel is transformed from curvilinear with positive curvature in subsonic profiles to rectilinear for transonic ones and of reverse (negative) curvature for supersonic ones, forming a divergent section from the throat to exit and in an uncovered outlet portion of the channel.

The reference [10] by F. W. Lipfert, discusses a method for profiling a supersonic nozzle with a one-sided divergent channel, like that presented in Figure 1d by M. E. Deich. For the subsonic section of the channel, [10] used a traditional approach based on the dependence of the channel camber line and the nozzle maximum thickness on the relative chord of the entire profile. Note that in this topology, the supersonic part of the channel is built with profiling only one side, namely the suction side wall, and does not correspond to the condition of minimal losses and a uniform velocity at the exit, as is ensured when profiling rocket nozzles. With this approach, it is possible to obtain relatively low values of Mach numbers due to the limitation on the channel divergent part design associated with one-sided profiling.

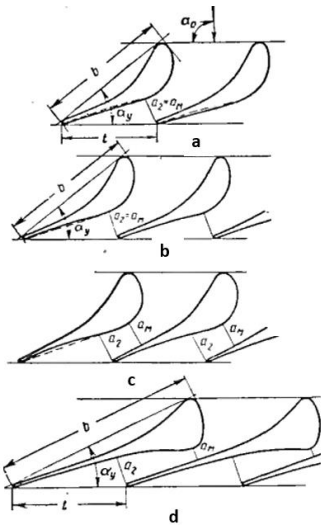

FIGURE 1: THE TYPICAL PROFILES FOR DIFFERENT MACH NUMBERS [24]

For subsonic profiles, several parametric models exist [15, 16, 19, 21]. As an example, the Pritchard model [15] consists of 11 parameters that completely determine the geometry of the profile. However, this model is based on a subsonic channel topology with a throat at the outlet and is not suitable for profiling either the subsonic part or the supersonic nozzle as a whole. For high-loaded turbine supersonic nozzles, the parametric models, accounting for above mentioned design features are not presented in the open literature, although some of the Pritchard model parameters were used in the developed nozzle model.

An analysis of publications on the development and testing of highly loaded supersonic turbines with high Mach numbers shows that the two different nozzle configurations are possible in terms of convergent part shape.

One variant of the inlet part of the channel uses the traditional radius type of the leading edge (Figure 2). In such a configuration the entire width of the channel pitch is used to pass flow inside [2, 3].

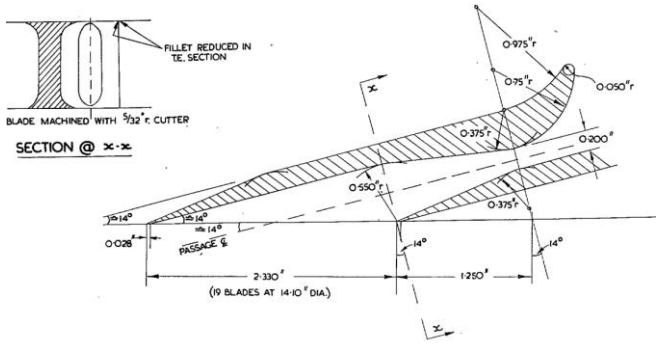

FIGURE 2: A CHANNEL FORMED BY BLADES WITH A RADIUS LEADING EDGE [2]

Another concept [4] of the nozzle inlet uses a straight-line segment (bridge) between leading edge arcs at both sides of the profile (Figure 3). This variant of the nozzle inlet reduces the channel inlet width, but improves the mechanical characteristics, increasing the area of the profile.

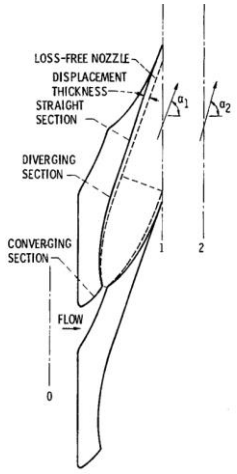

FIGURE 3: A CHANNEL FORMED BY BLADES WITH A THICKENED LEADING EDGE [4].

As mentioned above, in two high-loaded variants [2, 3, 4] the supersonic part of the channel is built by expanding both channel walls (suction side and pressure side) with continuation in the uncovered outlet, in contrast to the one-sided profiling method [15, 10]. In this case, the walls of the divergent section can be made either using a simplified approach (straight lines, Figure 2) or using special profiling methods, ensuring a minimum of losses in the divergent part of the channel (Figure 3).

Summarizing above we see such limitations in the open literature methods concerning the objective of this work:

- For highly loaded supersonic convergent-divergent nozzles, the concept of a chord as a basic parameter cannot be used since the topology of the supersonic channel differs from those of the subsonic ones. With the same subsonic part, the supersonic part can be of different configurations having different expansion ratios XPR and length L, thus affecting the total chord value. Therefore, the chord cannot be the base for constructing the subsonic part of the channel.
- Another aspect that is not considered in existing approaches is the formation of an inlet edge with a thickened part, which requires upgrading existing methodology or developing a new one.
- As for the expanding part of the channel, the method using one-sided profiling shown in Figure 1 does not allow obtaining large expansion ratios and is accordingly limited in Mach numbers. The developed method should be based on double-sided channel profiling using modern profiling methods like the ones used in rocket technology, to ensure high Mach numbers with minimal losses.

So, the following concept of a parametric model of the CDV nozzle is proposed and developed:

- The design model must contain a set of independent geometric parameters that, together with the input/output thermodynamic parameters and functions of the working fluid, uniquely determine the 3D geometry of the nozzle channel.
- Abandon the traditional concept of defining optimal whole profile parameters as a function of chord. Instead, to apply separate approaches to subsonic and supersonic part design.
- Organize the inlet part up to the throat, providing high aerodynamic characteristics using the discharge coefficient model.
- Organize a supersonic part with double-sided profiling, ensuring the possibility of high Mach numbers with a minimum of wave losses on the design mode of operation.
- Implement two options for the inlet edge within one model - a cylindrical leading edge (Figure 2), and thickened LE (Figure 3).
- By varying the width of the flat section of the inlet part and other parameters of the model, be able to change the mechanical properties of the profile section, thus adjusting the strength characteristics.
- Provide flexibility in ensuring turbine stage design criteria/constraints such as axial and tangential sizes, nozzle height, and number of nozzle channels in full circle (i.e. partial admission ratio, etc.) by varying nozzle model parameters.

1.2 Discharge coefficient.

Another important aspect of the design methodology is the influence of the channel geometry and flow regime on the discharge coefficient.

A large number of experimental and computational works have been devoted to the study of the features of supersonic flow in the critical throat section area [26-45]. In these works, the aspects influencing discharge coefficients are considered concerning both the geometry of the subsonic part of the channel and the flow regime. It should be noted that most of these works are devoted to the study of axisymmetric nozzles with a linear axis in both the inlet and outlet parts of the channel. Such nozzles are used primarily in rocket technology, and in a variety of technical applications, including Venturi-type flow meters with a critical flow regime. In general, the influence of two factors on the discharge coefficient was noted – the effect of the sound line Mach=1 curvature with deviation from the geometrical throat line and the boundary layer growth. Both of these factors depend on the shape of the subsonic section and the flow regime. In particular, the reference [26] showed the effect of the curvature of the walls on the shape of the sound line Mach=1 in the throat area. In [28, 37] conical variants of the axisymmetric nozzle were studied, and noted a significant influence of the conical angle of the inlet section on the discharge coefficient. Also, a strong effect of the wall curvature in the throat area was observed and investigated. The effect of the wall curvature radius is considered relative to the throat radius. For example, results obtained in [39]

show that an increase in the relative radius of the walls leads to a discharge coefficient decrease. It should be noted, that this result was obtained for relatively low Reynolds numbers in the range of 50-10^5 with the assumption of laminar flow. The proposed equation for C_d accounts for wall-to-throat radii ratio R_c/R_t, Reynolds number, and isentropic exponent.

$$C_d = 1 - (R_c/R_t)^{\frac{1}{4}} \cdot (1/Re)^{\frac{1}{2}} \cdot f(k) \qquad (3)$$

Studies [41, 42, 43] show the opposite effect, i.e. an increase in the discharge coefficient with an increase of wall curvature radius to throat radius ratio R_c/R_t. Figure 4 shows the data from [42] on the influence of the wall radius in jet engine nozzles, summarized data with different convergent area ratios and conical angles in front of the throat.

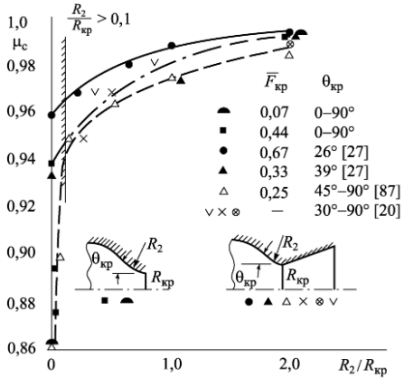

FIGURE 4: INFLUENCE OF RADIUS OF CURVATURE ON DISCHARGE COEFFICIENT [42]

In [43] the experimental data of Rao [44] for rocket engine nozzles were summarized with the same effect of wall curvature on discharge coefficient. The proposed formula [43] takes into account the radii ratio but does not account for the boundary layer via the Reynolds number function.

The formation and growth of a boundary layer on the walls and flow regime have been studied in numerous works [33-44]. This process is characterized by the Reynolds number [31, 34] and the roughness of the walls [35], which provide a significant effect on the discharge coefficient. For example, ASME PTC 19.5-2004 [33] summarizes a large number of experimental studies on Venturi flowmeter nozzles in a range of Reynolds numbers (1E4…1E7) and a generalizing dependence was obtained:

$$C_d = A - \frac{B}{\sqrt{Re_d}} \qquad (4)$$

where A=0.9959, B=2.72 and Re_d is the Reynolds number determined by the diameter of the cylindrical throat.

Some studies also note the influence of the real gas properties on C_d [35, 36].

The analysis of publications shows the complex nature of the dependence of the discharge coefficient on many geometric and flow regime parameters of supersonic nozzles. Two main contributors are - the geometry of the subsonic portion of the channel influences discharge coefficient via relative wall curvature. Another factor is boundary layer growth on the walls of the channel from the inlet to the throat. Boundary layer growth depends on several parameters – wall length, curvature, channel contraction ratio, roughness, and flow regime (laminar vs. turbulent), determined by Reynolds number. The final value of the discharge coefficient is the combined effect of these two main contributors.

In our case, we consider turbine-type channels that provide both acceleration of the flow and its turning in the tangential direction for subsequent acceleration to supersonic speed. In a turbine-type channel, the shape and, consequently, the wall curvature and length of the channel may strongly differ depending on the design requirements and are uniquely determined by a set of design parameters.

Analysis of the literature on discharge coefficient demonstrated that:

- In the open literature, there are recommendations for the selection of the discharge coefficients for traditional subsonic nozzles and axisymmetric supersonic rocket and Venturi types nozzles. However, there is no literature data on the discharge coefficient for turbine CDV-type nozzles.
- Dependencies used in rocket technology for calculating discharge coefficients cannot be directly applied to turbine profiles with the flow turn in the channel.
- Therefore, in this work, based on the described approaches for axisymmetric channels, a discharge coefficient calculation algorithm proposed and developed, that takes into account the multivariant geometric configurations of the turbine CDV nozzles, the height of the nozzle, and the flow regime parameters – Reynolds number and wall roughness.

2. PARAMETRIC MODEL OF THE CONVERGENT PART OF THE NOZZLE

The initial data for the supersonic nozzle profile design are the following parameters obtained at the turbine stage design step, preceding to profiling step:

- fluid properties - k and R for an ideal gas or thermodynamic properties for a real gas.
- G – the gas mass flow rate through the entire nozzle ring.
- D – mean diameter for which the nozzle is positioned.
- z – number of opened nozzle channels.
- pa – partial admission ratio.
- alpha – the nozzle axis angle to the circumferential direction.
- Total parameters in front of the nozzle and static pressure after P_0^* - Pressure and T_0^* - Temperature (or I_0^*- Enthalpy), P_s.
- r_2 – TE radius.

Some other parameters required for the profiling process are as follows:

- pitch at mean diameter

$$t = \frac{\pi \cdot D \cdot pa}{z} \qquad (5)$$

- mass flow rate per 1 channel

$$G_1 = G/z \quad (6)$$

- the nozzle outlet channel width

$$a_{exit} = fun(t, alpha, r_2) \quad (7)$$

- XPR is determined via the pressure ratio

$$XPR = fun(\frac{P_0^*}{P_s}, k) \quad (8)$$

- Critical throat $a_{cr} = a_{exit}/XPR$ (9)

- The critical throat area is determined with an accuracy of the flow coefficient C_d, which is unknown at the start of the design and depends on convergent part parameters. It could be assumed equal to 1.0 at the 1st iteration with refinement at the following iterative steps using the found convergent part parameters.

$$A_{cr} = \frac{G1}{c_{cr} \cdot \rho_{cr} \cdot c_d} \quad (10)$$

- Nozzle channel height

$$H = A_{cr}/a_{cr} \quad (11)$$

- Isentropic Mach number at the nozzle exit

$$M_t = fun(\frac{P_0^*}{P_s}, k) \quad (12)$$

Figure 5 shows the general scheme of a convergent-divergent channel with a set of parameters that unequivocally determine the configuration of the convergent part of the channel.

The construction begins with the critical throat size a_{cr}, whose direction is determined by axis angle alpha. The center point of the critical throat serves as the basis for the construction of the nozzle profile in both the convergent and divergent parts.

To build a parametric model of the converging part, the following parameters are used:

- r_1 is the radius of the inlet edge,
- H_{ax} is the distance from the center of the critical throat to the center of the leading edge in the axial direction.
- H_{tan} is the distance from the center of the critical throat to the center of the inlet edge in the circumferential direction.
- phi_{ss} and phi_{ps} are wedge angles at both sides of the channel - suction and pressure side.
- The suction and pressure side of the channel are formed by controlled cubic Bezier splines, which are tangent to the LE radius with angles phi_{ss} and phi_{ps} accordingly. Other splines end connects normally to critical throat ends accordingly.
- In addition to this set of parameters, one more input parameter has been introduced – the convergence factor (Figure 5.)

$$conv = \frac{A_{in} - A_{in\_min}}{t - A_{in\_min}} \quad (13)$$

where $A_{in\_min} = a_{cr} + 2 \cdot r_1$ (14)

This parameter characterizes the decrease in the contraction ratio of the channel from the inlet to the critical throat, caused by the enlarged width of the LE. With this parameter at $conv$=1 the inlet part has the traditional radius type of LE, and with $conv$ <1.0 forming the inlet part with a thickened LE, as in Figure 5.

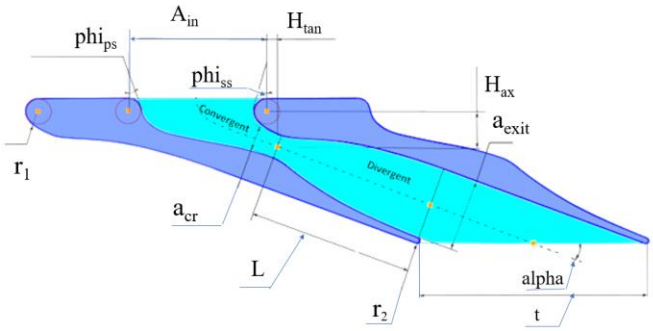

FIGURE 5: THE CONVERGENT-DIVERGENT CHANNEL WITH THE MAIN DESIGN PARAMETERS

The specified parameters r_{1_rel}, H_{ax_rel}, and H_{tan_rel} in the parametric model are dimensionless and are related to the value of the critical throat a_{cr}. These parameters, together with the wedge angles phi_{ss} and phi_{ps}, alpha, conv, and pitch t allow unambiguously to form the configuration of the convergent part. The set of these parameters determines and controls the curvature and length of the channel walls and is used as variables in the development of the nozzle discharge coefficient model.

Figure 6 illustrates the flexibility of the model and shows a variety of configuration options for the converging portion as the design parameters change. The optimal combination of parameters, which corresponds to the condition of the highest possible flow coefficient on the one hand, satisfying structural requirements and the design constraints on dimensions on the other, could be determined with this parametric model.

3. A SUPERSONIC EXPANDING PART OF THE CHANNEL.

For the design of the divergent portion of the supersonic channel, the method of characteristics MOC for ideal gas [45,46,47] is utilized, which is widely used in the aerospace industry. These methods make it possible to design the contours of the supersonic section with minimal losses and the most uniform flow output from the nozzle.

The two approaches were used to design the supersonic section of the nozzle channel:

- method of characteristic (MOC);
- simplified variant with splines - Bell type.

The first variant of the supersonic channel is performed according to MOC for an ideal gas under the assumption of a

straight sound line coinciding with the geometric throat (Figure 7).

The second variant is the BELL-type channel uses a controlled cubic Bezier spline. In this variant, the spline is connected to the throat line by a transition arc with angle phi=f(M_t) and radius R_c=f(a_{cr}) (Figure 8).

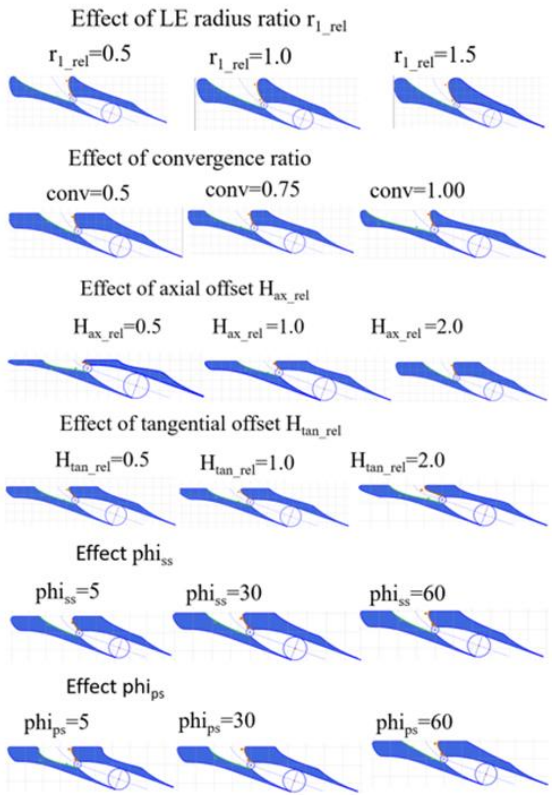

FIGURE 6: CHANNEL CONFIGURATION OPTIONS WHEN CHANGING THE MODEL PARAMETERS WITH OTHERS FIXED (r_{1_rel}=0.5, conv=0.75, H_{ax_rel}=1.0, H_{tan_rel} =1.0, phi_{ss}=30 deg, phi_{ps}=30 deg)

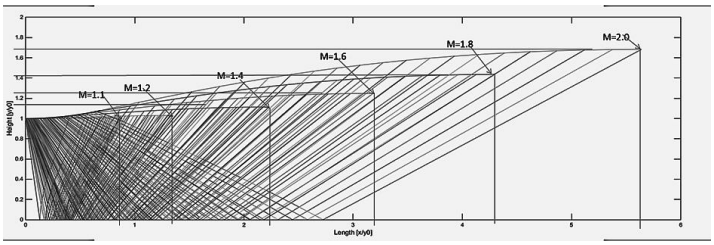

FIGURE 7: THE NOZZLE CONTOUR DESIGN ACCORDING TO MOC AND COMPARISON OF CONTOURS AT DIFFERENT MACH NUMBERS (K=CP/CV=1.4)

The length of the expanding part of the channel L=f(M_t) as well as transitional arc angle phi=f(M_t) and radius R_c=f(a_{cr}) in the BELL-type variant is determined from the preliminary calculation using the MOC method for the assigned XPR and k.

For both MOC and BELL types, the suction side of the channel continues as a straight line from exit to outlet at alpha angle, forming the outlet uncovered portion of the channel.

For the supersonic section of the channel, a length factor L_d is introduced:

$$L_d = \frac{L}{L_{ideal}} \tag{15}$$

which shows how much the real divergent part length differs from the ideal length. In this way the profiling process allows more flexibility to satisfy the design constraints of the turbine design as it is widely used in the aerospace industry [42].

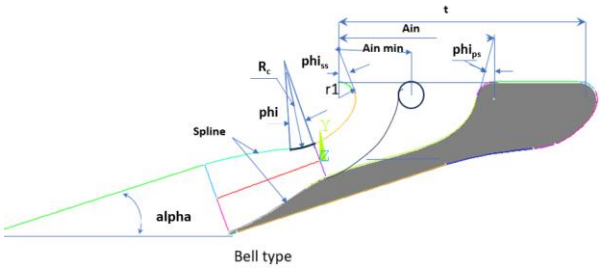

FIGURE 8: THE BELL-TYPE CDV NOZZLE VARIANT

Figure 9 shows two variants of the supersonic (divergent) part.

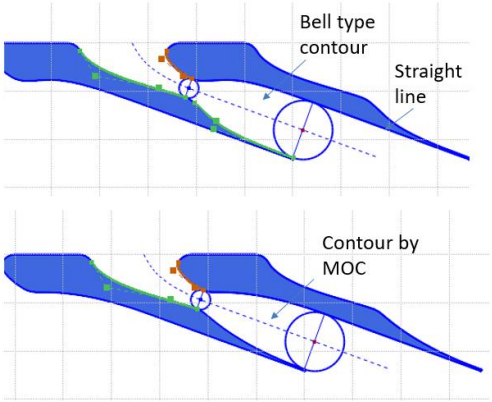

FIGURE 9: THE TWO VARIANTS OF THE SUPERSONIC SECTION OF THE CHANNEL – BELL TYPE AND MOC METHOD

The profile model considers the two types of trailing edge configuration: Cut-off type and Radius type.

4. 3D (SPATIAL) MODEL OF THE CHANNEL

When designing a turbine stage, the supersonic profile technique described above is used for several cross-sections along the nozzle height.

Two approaches were applied for the 3D design of the nozzle channel and implemented into the turbine design tool. One approach is to maintain the same expansion ratio (XPR=Const) in each cross-section along the nozzle height. In our case, we consider three cross sections at 0, 0.5, and 1.0 span

along the height. In this case, the critical throat, outlet channel width, and pitch change proportionally to the section radius.

The second approach takes into account the variable pressure drops at each radius along the nozzle height, which decreases from the hub to the shroud. The pressure difference between the shroud and hub could be determined from a simplified radial equilibrium equation.

$$Delta\ P = P_{shroud} - P_{hub} = \int_{R_{hub}}^{R_{shroud}} \frac{\rho C_u^2}{R} dR \qquad (16)$$

In this case, the design of the supersonic part is performed with a variable expansion ratio (XPR=Var.) along the radius determined by the respective pressure ratio. The difference in XPR values between the hub, middle, and shroud sections, in this case, depends on the relative height of the blade. This variant allows better adjustment of nozzle expansion ratio XPR to respective pressure drop at each span thus decreasing losses, associated with off-design performance at each span location. It should be noted that the effect of two different XPR approaches does not affect on discharge coefficient and is not analyzed in the scope of this article.

Figure 10a demonstrates the contours of the channels in different cross-sections (XPR=Const) which are shown in different colors. Figure 10b shows the 3D geometry of the blades. When building 3D blade geometry, the profile coordinates obtained for planar sections are converted to cylindrical surfaces. The obtained 3D geometry can be exported into external programs (CAD, FEA, CFD) for further design steps.

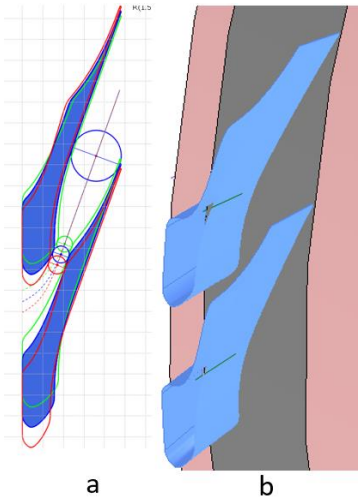

FIGURE 10: A - CHANNEL PROFILES IN THREE CROSS-SECTIONS AND B - 3D BLADE GEOMETRY

The 3D nozzle design requires the coordination of the individual profile's positions at each cross-section relative to the radius vector – stacking. In our design method, 3 variants of stacking are used – by the center of the trailing edge, by the critical throat center, and by the center of the leading edge. Each variant allows the designer to create a three-dimensional version of the nozzle vanes per preferences for the design of the turbine.

The above-mentioned set of parameters uniquely determines the 3D geometry of the nozzle channels and corresponding vanes in both the subsonic and supersonic parts of the channel, which makes it possible to store a set of specified parameters instead of all detailed 3D geometry, thus reducing project information.

5. SUPERSONIC CHANNEL DISCHARGE COEFFICIENT AND APPROACHES TO ITS DETERMINATION

When designing highly loaded turbines with supersonic flow regimes, the correct determination of the discharge coefficient is necessary to determine the size of the nozzle for the working fluid MFR specified for the design. An error in the discharge coefficient results in a proportional error in turbine power, size, and weight, which can be critical for aerospace and other applications.

In this work we consider the influence of two effects noted in the literature review on the discharge coefficient: the influence of the curvature of the channel from the inlet to the throat on the sound line deviation from the geometrical throat, and the influence of the accumulated boundary layer.

The actual flow rate of a supersonic nozzle channel is determined using the discharge coefficient, which is the ratio of the actual flow through the channel to the theoretical (ideal) flow rate.

$$C_d = \frac{G}{G_{ideal}} \qquad (17)$$

The theoretical flow rate is determined under the assumption of isentropic adiabatic flow using critical parameters – velocity, density, and area of the critical cross-section:

$$G_{ideal} = A_{cr} \cdot C_{cr} \cdot \rho_{cr} \qquad (18)$$

$$C_{cr} = \sqrt{\frac{2kRT_0^*}{k+1}} \qquad (19)$$

$$\rho_{cr} = \left(\frac{2}{k+1}\right)^{\frac{1}{k-1}} \rho_0^* \quad \text{, where} \qquad (20)$$

$$\rho_0^* = \frac{R \cdot T_0^*}{P_0^*} \qquad (21)$$

By the nature of supersonic flow in a convergent-divergent nozzle at a supercritical pressure drop, the flow rate does not depend on the pressure variation downstream nozzle and is determined by the flow coefficient.

6. EFFECT OF CHANNEL WALL CURVATURE ON DISCHARGE COEFFICIENT.

To study the effect of wall curvature on the sound line Mach=1 deviation from the geometrical throat line, a series of 7 convergent-divergent channels with axis angles varying from 8 to 20 degrees were designed in two variants: with the same pitch (Figure 11a), giving a variable critical throat size from 1.9 mm to 4.07 mm, and with the constant critical throat size of 4.07 mm (Figure 11b). The input parameters were taken Pt=48 bar and Tt=753 K with a pressure ratio of 21.1, which corresponds to XPR=3 for all variants.

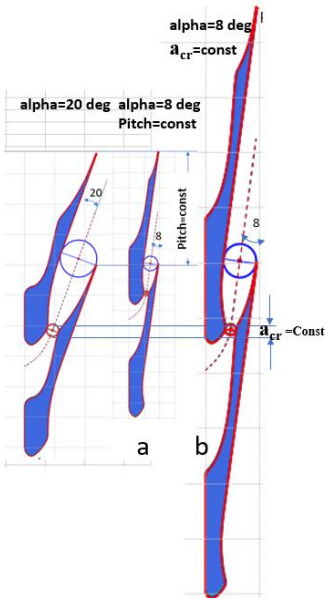

FIGURE 11: COMPARISON OF PROFILES WITH 20- AND 8-DEGREE AXIS ANGLES THROAT=VAR (a) AND THROAT=CONST (b)

These parameters are typical, particularly, for high-loaded water pump drive turbines where the developed nozzle could be implemented. The values of the Reynolds numbers, calculated by the throat, are in the range from 7.2E5 to 15.5E5.

CFD calculations were performed in ANSYS CFX. Figure 12 shows a pseudo-2D CFD model of the nozzle. The blade surface was a rough wall with 5 µm equivalent sand grain roughness. The end walls were defined as symmetry walls to exclude friction. The working fluid is air modeled as an ideal gas. In the CFD model, a hexahedral mesh was used with a boundary layer created to have a y+ <20 condition on the surface of the blade. The k-omega SST turbulence model with 5% turbulence intensity and viscosity ratio=10 at the inlet was used in all series of calculations [49].

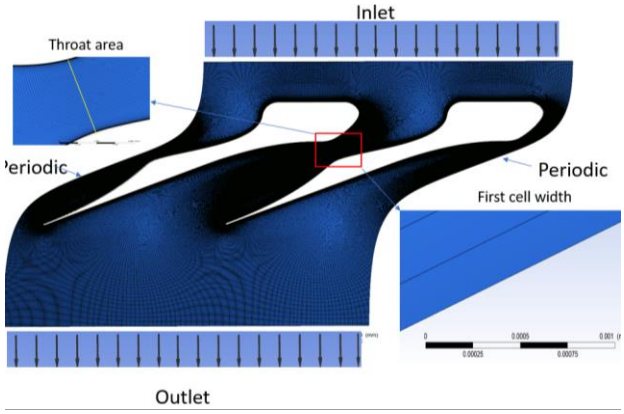

FIGURE 12: CFD MODEL FOR CALCULATION OF DISCHARGE COEFFICIENTS

Figure 13 shows the relative deviation of C_d in the studied model depending on the number of grid cells. Four variants of sensitivity calculations with grids with 0.3, 1.0, 2.0, and 4.0 million cells were performed. The y+ parameter, averaged for blade surface, corresponding to different grid sizes was 107, 37, 15, and 10 accordingly. Two variants of nozzles with axis angles of 8 deg and 20 deg. have been studied. Relative C_d deviation is shown as a percentage of the C_d level with a maximum cell count of 4.0 million for both axis angles. For further calculations, a variant of the grid with 2.5 million elements was adopted, where parameters were stabilized.

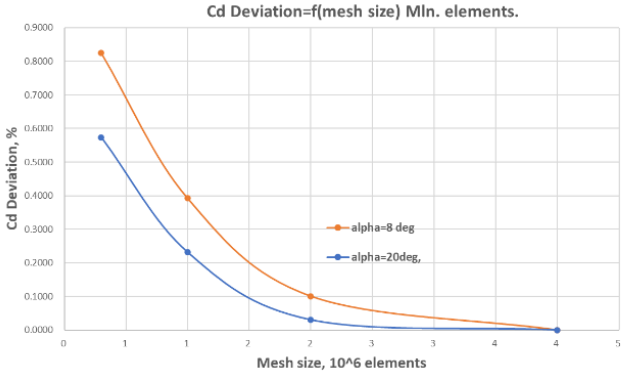

FIGURE 13: SENSITIVITY OF THE FLOW COEFFICIENT CALCULATION TO THE MESH DIMENSION

In order to separate the effects caused on one side by the curvature of the channel and on the other by the boundary layer growth, each of these series was studied with free slip walls to exclude the boundary layer and with blade walls of 5 µm equivalent sand grain roughness for boundary later simulation.

Calculations with free-slip walls made it possible to isolate the effect of wall curvature on the flow coefficient C_{d_slip}, and calculations with rough walls made it possible to obtain the total effect on the flow coefficient C_d. In both series, the curvature of the channel walls in proportion to the throat radius R_c/R_t with $R_t=a_{cr}/2$ were analyzed (Figure 14). Since the radii of curvature on the pressure side are much larger than that on the suction side, the analysis was performed only for the suction side. Figure 14a shows a variant with a variable throat and constant pitch, and Figure 14b – is a variant with variable pitch and constant throat.

The chart in Figure 15 compares two variants of channel formation concerning the effect on wall maximum radii ratio R_c/R_t. For variant *throat =Var* the ratio R_c/R_t increases as alpha decreases from 20 deg to 8 deg. Variant *throat=Const* shows the opposite trend.

Figure 16 shows how the discharge coefficients depend on the R_c/R_t ratio for both variants of geometry formation. The upper lines show the free slip walls variant C_{d_slip} and the bottom lines variant C_d with a boundary layer. Both variants support the effect for C_{d_slip} increase with an increase in R_c/R_t ratio, which is consistent with the conclusions from [39]. Whereas bottom C_d lines show the opposite trend concerning the R_c/R_t ratio. This result could explain different trends, referenced in [36] and in

[39, 40], which most likely relate to different conditions for boundary layer development.

In the current study, such difference could be explained by different conditions of boundary layer growth, resulting from different channel lengths, curvature, and contraction ratio, which is seen in Figure 16.

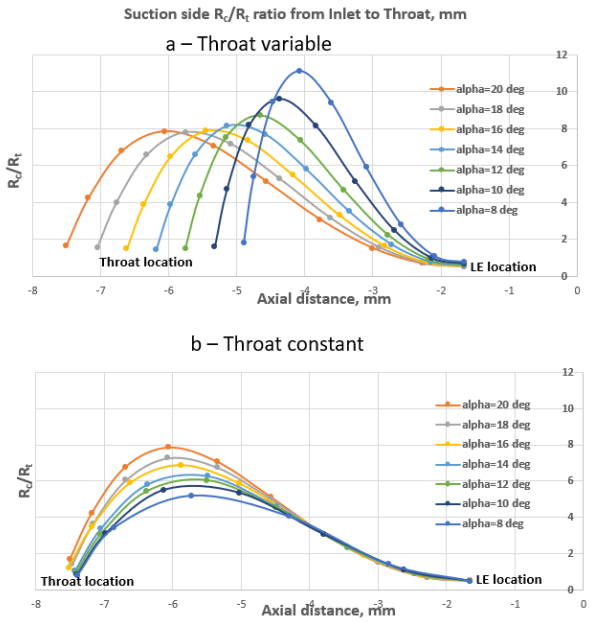

FIGURE 14: DISTRIBUTION OF THE RELATIVE RADIUS OF CURVATURE RC/RT ON THE SUCTION SIDE OF THE NOZZLE CHANNEL

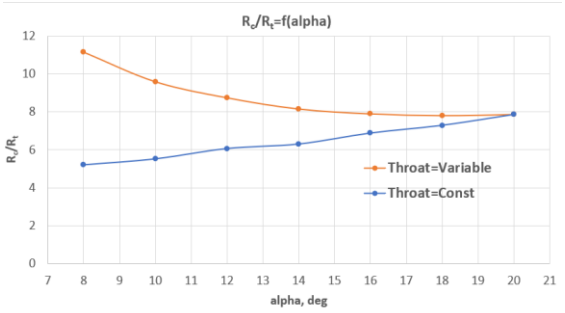

FIGURE 15: DISTRIBUTION OF MAXIMUM RELATIVE RADIUS RC/RT FOR TWO VARIANTS OF CHANNEL FORMATION

As a conclusion from this study, the discharge coefficient model for turbine convergent-divergent channel with a variety of potential channel shapes, cannot be modeled accounting only for relative walls maximum curvature R_c/R_t as a main influencing parameter and should consider more factors, such as:

- the shape of the inlet part of the channel (including the axis angle of the channel), which affects the length and curvature of the walls;
- the influence of the flow mode expressed as dependence on the Reynolds numbers and the roughness of the channel walls;
- relative height of the channel, to account for the effect of the end walls losses.

Based on the above conclusion, the following variant of C_d dependency is proposed:

$$C_d = (C_{d\_base} - \Delta C_{d\_Re}) * K_{Roug} * K_{H\_rel} \quad (22)$$

Here C_{d_base}, instead of a fixed value like in [30] is defined as a function of 7 variables, responsible for the shaping of the convergent portion of the channel.

$$C_{d\_base} = f(r_{1\_rel}, conv, H_{ax\_rel}, H_{\tan\_rel}, phi_{ss}, phi_{ps}, alpha) \quad (23)$$

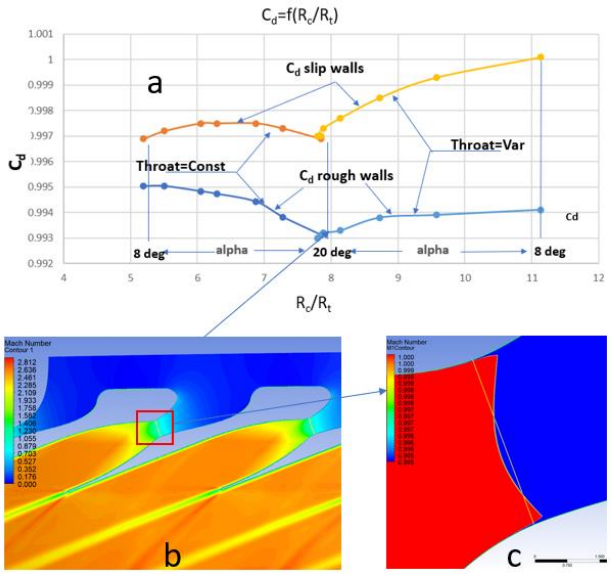

FIGURE 16: DEPENDENCE OF DISCHARGE COEFFICIENTS ON R_c/R_t FOR THROAT=VAR AND THROAT=CONST (a); FLOW FIELD IN CHANNEL (b) AND SOUND LINE MACH=1 VS THROAT LINE (c)

The effect of the Reynolds number is taken into account by the correction function $\Delta C_{d\_Re} = f(Re)$.

Two additional correction factors are:

- K_{Rough} – the effect of roughness,
- K_{H_rel} – the effect of the relative height of the channel in proportion to the critical throat.

7. BASE DISCHARGE COEFFICIENT MODEL USING SURFACE RESPONSE METHOD.

In order to obtain the C_{d_base} as a function of 7 independent parameters, the Response surface methodology was selected with the use of the DOE Box–Behnken plan [48] approach.

The essence of this approach is that each factor is given at three equally spaced levels, usually coded as −1, 0, +1. With 3 levels of variables, the resulting function will be quadratic with

additional terms that take into account the cross-influence of the parameters.

In our case, 7 variables normalized in the range -1, 0, +1 are presented in Table 1.

TABLE 1: DOE INDEPENDENT PARAMETER LEVELS

	r_{1_rel}	conv	H_{ax_rel}	H_{tan_rel}	phi_{ss}	phi_{ps}	alpha
Min	0.5	0.2	1	0.45	15	15	8
Mid	1	0.6	2	0.75	45	45	14
Max	1.5	1	3	1.5	60	60	20

When choosing the range of physical parameters between min and max, a study was carried out on the influence of all parameters involved in the profiling on the following aspects:

- gas-dynamic characteristics of the inlet section, i.e. providing adequate convergence of the channel from the inlet to the throat to avoid the degraded shape of the channel, as shown in (Figure 17a).
- the range of parameters was analyzed from the point of view of excluding the intersection of the contours of the SS and PS with each other, as shown in (Figure 17b).
- the H_{ax} parameter was limited by the maximum value to avoid increasing the axial size of the nozzle in terms of excessive metal consumption, as shown in (Figure 17c).
- The mechanical characteristics of the profile cross-section, such as profile area, moments of resistance and moments of inertia, and other parameters involved in the strength calculation were analyzed. Comparison of these characteristics in the range between min and max showed their difference by more than 3 times, which makes it possible to effectively adjust strength criteria for the design of a turbine stage.

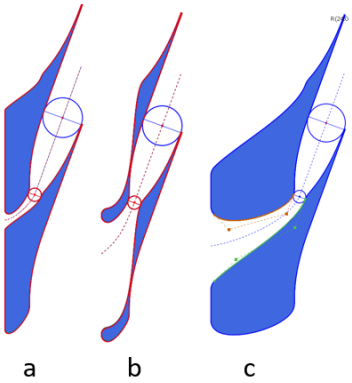

FIGURE 17: VARIANTS OF UNDESIRABLE NOZZLE CHANNEL SHAPE

Wall curvature radii R_c/R_t ratio and profile shape, corresponding to the Min, Mid, and Max parameters range are changing significantly, as shown in Figure 18, thus influencing discharge coefficients. Hence accepted DOE range of parameters covers a broad variation of profile shape concerning wall curvature R_c/R_t ratio and mechanical characteristics, that could be met in design practice.

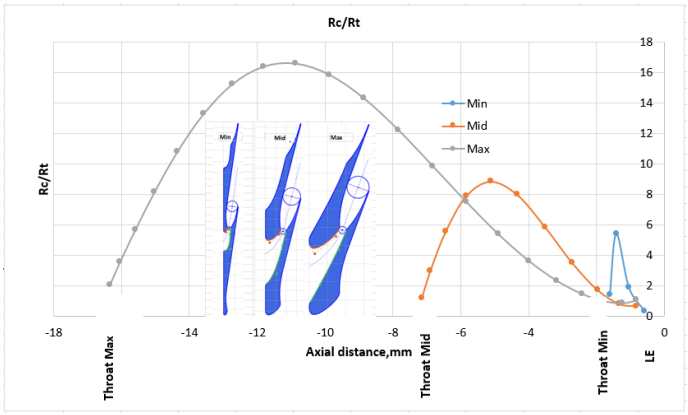

FIGURE 18: PROFILE SHAPE, CORRESPONDING TO MIN, MID, AND MAX PARAMETERS

The total number of calculations according to the Box–Behnken plan was 62 and the number of coefficients with a full quadratic regression model, taking into account the effects of the interaction of all 7 parameters, is equal to 36. General view of a complete quadratic model:

$$y = b_0 + \sum_{i=1}^{n} b_i x_i + \sum_{i=1}^{n} b_{ii} x_i^2 + \varepsilon \qquad (24)$$

where linear, quadratic, and pairwise terms ε are involved.

Dependency for Cd_{base} is obtained as a result of a series of the CFD model calculations, with the following parameters: *Re =2.67E+6*, blade wall roughness 5 μm, and free slip end walls, which exclude the influence of the channel height and the secondary flow losses.

The entire series of DOE plan runs were performed in ANSYS CFX with the same methodology as the first series of CFD calculations described above. Taking into account the large volume of calculations, the entire process was automated with the construction of channel geometry in the turbine design program for each of the plan options, and further CFD calculation in ANSYS CFX. The CFX results for all runs, were processed by SoftInWay Inc. company proprietary program to obtain a regression equation.

Figure 19 shows the distribution of relative deviations of the regression model from CFD calculations for all DOE plan variants.

The average standard deviation percentage for the entire plan is $S = 0.18\%$ and the coefficient of determination of the quadratic fitting $R^2 = 0.727$.

Analysis of the distribution of deviation values at all points of the plan (Figure 20), shows good adequacy of the model.

The parameters of the optimal profile in the studied DOE range and the values of the predicted vs. CFD discharge coefficients C_d are shown in Table 2 and FIGURE 21. The deviation of the predicted value from CFD is 0.18%. FIGURE 21 shows the shape of the designed optimal profile (a), the Mach number (b), and the position of the sound line Mach=1 (c) relative to the geometric throat. As it can be seen the isoline Mach=1 is located in the area of the geometric throat of the

nozzle. However, it has distinct curvature, which is the consequence of flow turn in the subsonic part of the nozzle.

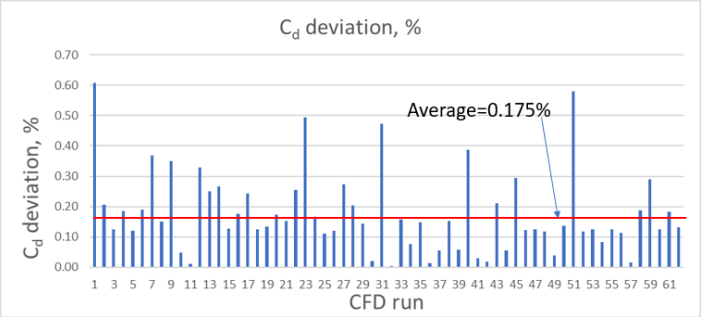

FIGURE 19: RELATIVE DEVIATION DISTRIBUTION FOR THE ENTIRE DOE PLAN.

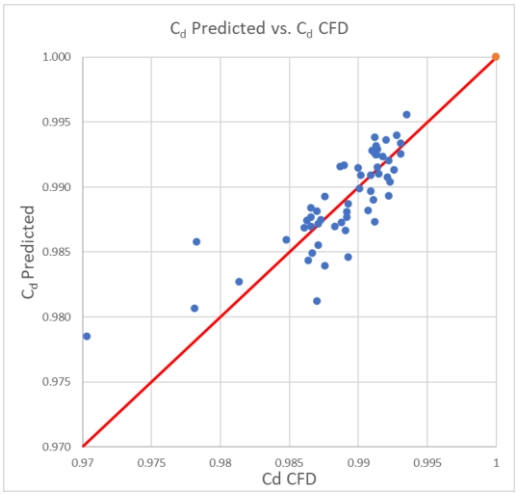

FIGURE 20: COMPARISON OF THE PREDICTED C_d COEFFICIENTS OF THE MODEL WITH THE RESULTS OF THE CFD CALCULATION

TABLE 2: THE SUBSONIC PART OPTIMAL PARAMETERS AND RESPECTIVE CD VALUES

Param	r_{1_rel}	conv	H_{ax_rel}	H_{tan_rel}	phiss	phips	alpha	C_d pred*	C_d CFD	dev, %
Value	1.5	0.6	2	0.75	45	15	20	0.9956	0.9938	0.18

* C_d pred stands for discharge coefficient predicted by the proposed model

8. EFFECTS OF REYNOLDS NUMBER, ROUGHNESS, AND RELATIVE HEIGHT IN THE MODEL.

Effect Reynolds and Roughness on Cd.

To obtain different Reynolds numbers the pseudo-2D CFD model has been scaled down and analyzed at constant inlet conditions, 5 µm roughness, and pressure ratio at *XPR= 3*. Reynolds numbers vary in the range 0.2E5 – 8.0E6. These results were used to derive the $\Delta C_{d\_Re} = f(RE)$ correction function. The normalized correction function $\Delta C_{d\_Re} = f(RE)$ is shown in FIGURE 22. This figure also shows the dependence of the discharge coefficient on the Reynolds number obtained for Venturi nozzles [33]. The chart shows a weaker influence of the Reynolds number in the case of CFD calculations. This could be explained by the fact that in the case of Venturi nozzles, friction occurs over the entire surface of the channel, and the Reynolds number is determined by the diameter of the nozzle throat. In the case of the CFD model of the CDV nozzle, friction was modeled only on the blade walls and was not modeled on the end walls, and the Reynolds number was determined by the linear size of the throat. In the proposed Cd model the effect of end wall friction is accounted for separately by introducing a relative height correction factor.

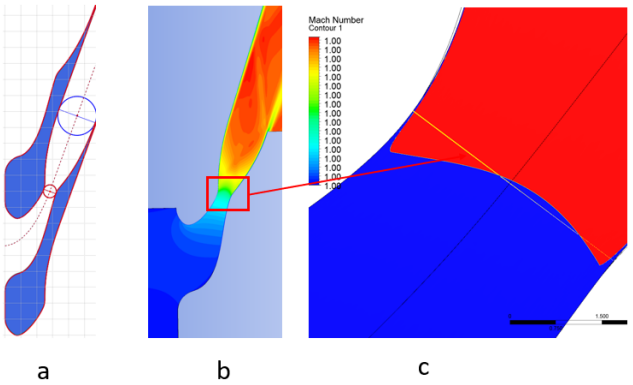

FIGURE 21: OPTIMAL PARAMETERS AND COMPARISON OF PREDICTED DISCHARGE COEFFICIENT AND CFD RESULTS

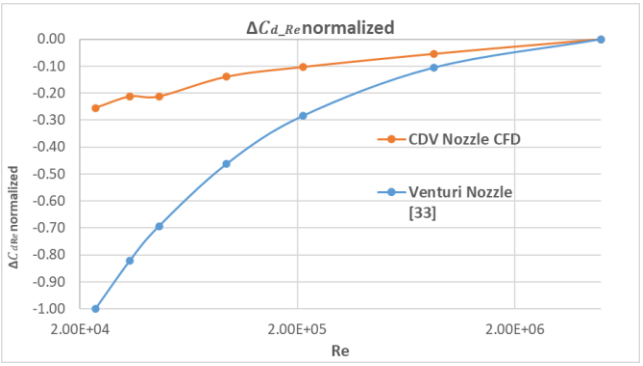

FIGURE 22: ΔC_{d_Re}=F(RE) CORRECTION FUNCTION

In addition to the Reynolds correction function, the effect of roughness is taken into account by modeling three roughness levels Rs= 0 µm, 5 µm, and 14 µm with a fixed value of the Re=5.0E6. These three levels of roughness represent variants of the ideal, average, and coarse levels of machining. The roughness correction factor $K_{Roug} = f(Roughness)$ is shown in FIGURE 23.

Effect of Relative Height on Cd

The K_{H_rel} correction factor takes into account the effect of the relative height of the channel on the C_d. 5 series of CFD calculations with different design pressure ratios (PR=5…50) and with 6 different relative height H_{rel} values were performed.

H_{rel} parameter vary from 1 to 30 and covers a broad range of nozzle heights, which could be met in design practice.

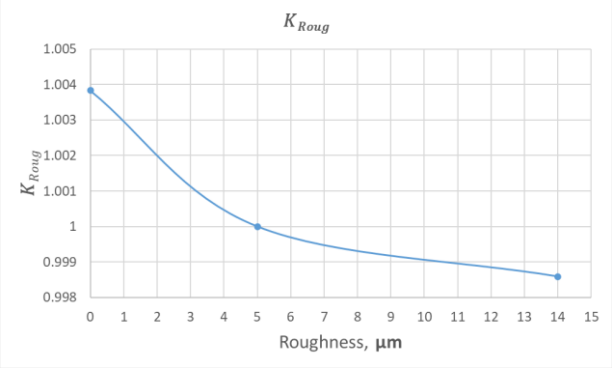

FIGURE 23: K_{Roug} CORRECTION FACTOR

The 3D nozzle vanes were designed in turbine design software and exported to ANSYS CFX. The 3D CFD model represents a linear 3D cascade with 5 **µm** roughness at blades and end wall surfaces.

FIGURE 24 shows the normalized correction factor K_{H_rel} as a function of relative height $H_{rel}=H/a_{cr}$.

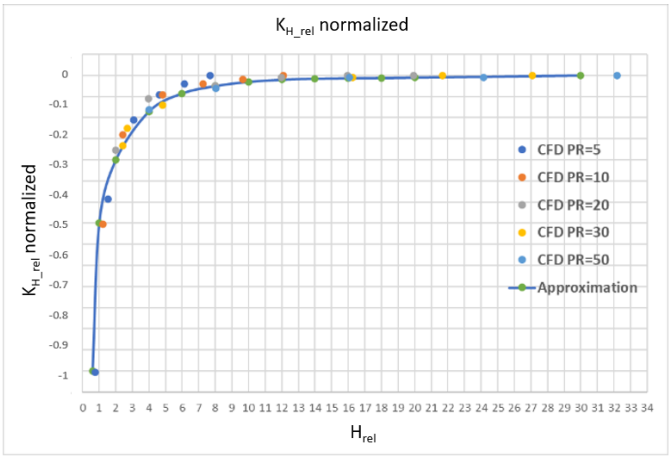

FIGURE 24: CORRECTION FACTOR K_{H_rel} AS A FUNCTION OF THE RELATIVE HEIGHT H_{rel}

9. VALIDATION

Validation of the obtained model was carried out on 7 variants of the turbine nozzle 3D CFD circular cascade models, built according to a combination of geometric and regime parameters different from those used in the development of C_d (22) and C_{d_base}(23). All nozzle variants are designed in the AxSTREAM® tool and exported to CFX to obtain C_d reference values. FIGURE 25 shows the variants of profile shape (a) with a different combination of parameters for the convergent part of the channel, different heights in the range 8mm-60mm, and angles in the range 8-20 degrees. Roughness also varied in the range of 5 µm – 14 µm. FIGURE 25 also shows variant 3 circular cascade Mach number field (b). All variants have the same inlet parameters and the same XPR for divergent parts of the channel.

Tables 3 and 4 show the characteristics of the models, the referenced Cd values obtained in CFD, and the predicted C_d values. C_{d_base} obtained from the 7 geometric parameters of the convergent part are presented in Table 3. C_d accounting for C_{d_base} and effects of Reynolds number, roughness, and relative height H_{rel} of the vanes, are presented in Table 4.

The tables also show the relative deviation from CFD values for both variants of predicted values, which are at the same level of accuracy of 0.02-0.17% for C_{d_base} and for C_d.

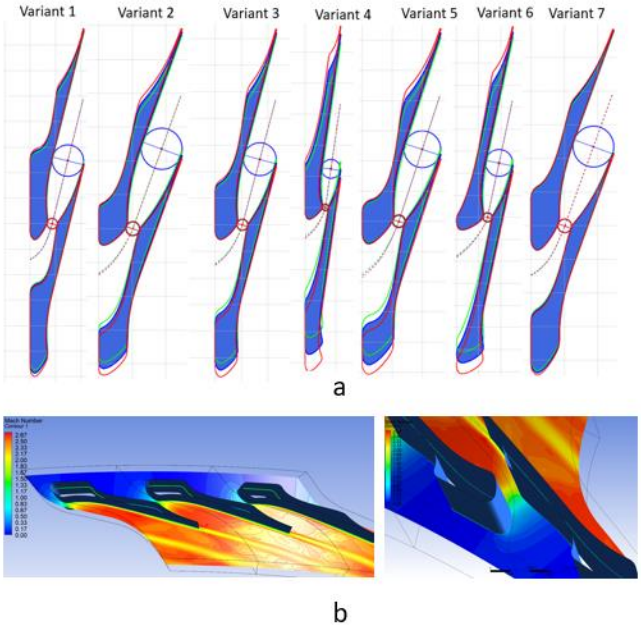

FIGURE 25: 7 VARIANTS OF PROFILES, USED FOR VALIDATION (a) AND VARIANT 3 CIRCULAR CASCADE FLOW FIELD (b)

TABLE 3: C_{D_BASE} DISCHARGE COEFFICIENT VALIDATION

Var.	r_{1_rel}	conv	H_{ax_rel}	H_{tan_rel}	phi_{ss}	phi_{ps}	alpha	Cd_{base} CFD	Cd_{base} pred	dev, %
1	1	0.3	1.1	0.75	45	15	14	0.9922	0.9933	0.111
2	0.5	0.7	2	0.75	45	25	20	0.9928	0.9911	0.171
3	1	0.6	1.5	0.55	45	30	15	0.9922	0.9929	0.071
4	1.5	0.6	1.75	0.75	50	60	8.23	0.9892	0.9908	0.162
5	1	0.75	2	1	45	15	18.07	0.9934	0.9950	0.160
6	1.25	1	2.2	0.5	55	60	12	0.9888	0.9879	0.091
7	1	0.5	1.35	1	55	30	20	0.9929	0.9916	0.131

TABLE 4: C_D DISCHARGE COEFFICIENT VALIDATION

Var.	Re	Roughness, µm	Height, mm	H_{rel}	Cd CFD	Cd pred	dev, %
1	3.00E+06	5	12	2.92	0.9899	0.9894	0.046
2	4.33E+06	7	25	6.16	0.9913	0.9907	0.058
3	4.33E+06	5	25	6.06	0.9916	0.9905	0.107
4	6.71E+06	14	60	14.79	0.9890	0.9873	0.172
5	5.12E+06	5	35	8.62	0.9931	0.9947	0.166
6	5.48E+06	10	40	9.80	0.9878	0.9865	0.132
7	2.45E+06	5	8	1.97	0.9845	0.9856	0.116

10. CONCLUSION

The analysis of existing publications in the public domain concerning supersonic convergent-divergent vaned nozzles showed that for such nozzles, the concept of a chord as a basic parameter cannot be used since the topology of the supersonic channel differs from those of the subsonic ones. With the same subsonic part, the supersonic part can be of different configurations having different expansion ratios and lengths, thus affecting the total chord value. Therefore, the chord cannot be the base for constructing the subsonic part of the channel. Besides, the thickened inlet edge is not considered in the existing approaches, which require upgrading the methodology or developing a new one. Further, the utilization of the one-sided profiling of the supersonic nozzle section does not allow obtaining large expansion ratios and is accordingly limited in Mach numbers.

The flexible parametric model of the supersonic channel and corresponding nozzle vanes was developed that enables the attainment of the desired flow parameters and high efficiency while satisfying structural constraints. The parametric model includes the design of the subsonic section with round and thickened leading edge types using the discharge coefficient model and the supersonic part using double-sided profiling ensuring the possibility of high Mach numbers with a minimum of shock wave losses on the design mode of operation. The developed parametric model also accounts for the 3D spatial design of the nozzle vanes variants with constant and variable expansion ratios in a spanwise direction.

In this work, a discharge coefficient calculation model was proposed, developed, and incorporated into the AxSTREAM®. The model takes into account the multivariant geometric configurations of the turbine CDV nozzles, the height of the nozzle, and the flow regime parameters – Reynolds number and wall roughness.

The comparison of the discharge coefficient predicted by the developed model with CFD results for the convergent-divergent vaned nozzles showed a good agreement.

The utilization of the developed parametric profiling model and the discharge coefficient prediction model provides the opportunity to design highly efficient supersonic turbines with convergent-divergent vaned nozzles.

ACKNOWLEDGEMENTS

We wish to thank the many people from the SoftInWay, Inc. team who generously contributed their time and effort in the preparation of this work. The strength and utility of the material presented here are only as good as the inputs.

REFERENCES

[1] Thomas P. Moffitt. Design and experimental investigation of a single-stage turbine with a rotor entering relative Mach number of 2. // Lewis Flight Propulsion Laboratory Cleveland, Ohio, 1958

[2] I. H. Johnston and D. C. Dransfield. The Test Performance of Highly Loaded Turbine Stages Designed for High-Pressure Ratio // Ministry of aviation London: her majesty's stationery office, 1959, Reports and Memoranda No.3242

[3] B. S. Stratford and G. E. Sansome. The performance of supersonic turbine nozzle // Ministry of Aviation London: Her Majesty's stationery office, 1962, Reports and Memoranda No.3273

[4] L. J. Goldman. Supersonic Turbine Design and Performance. GT Division of the ASME at the Gas Turbine and Fluids Engineering Conference & Products Show, San, Calif., March 26-30, 1972

[5] Linhardt H.D., Silvern D.H. Analysis of partial admission axial impulse turbines // ARS Journal. 1961.

[6] Barber R. E., Schultheiss M. J., Effect of nozzle geometry on the off-design performance of partial admission impulse turbine. Sundstrand Aviation division of Sundstrand Corporation. - 1967

[7] R. S. Peterson, S. C. Paskevich. An experimental study of nozzles and specific heat ratio effects on off-design performance of partial admission turbines. Sundstrand Aviation division of Sundstrand Corporation Rockford, Illinois, 1971

[8] Huzel D.K., Huang D.H. Modern engineering for design of liquid-propellant rocket engines. American Institute of Aeronautics and Astronautics - 1992.

[9] Daniel J. Dorney*, Lisa W. Griffin, Frank Huber, Douglas L. Sondak. Off-Design Performance of a Multi-Stage Supersonic Turbine. NASA Marshall Space Flight Center Applied Fluid Dynamics Analysis Group, 2003.

[10] Lipfert, F. W.; Fruchtman I. Design and development of supersonic turbine nozzle. National Technical Reports Library. Technical Report, AD901525

[11] L. Moroz, M. Burlaka, A. Yudin Influence of the convergent-divergent nozzles arrangement parameters on aerodynamic losses and overall supersonic turbine performance. - Proceedings of ASME Turbo Expo 2022 Turbomachinery Technical Conference and Exposition GT2022.- GT2022-83387 -2022.

[12] Aki Grönman, Teemu Turunen-Saaresti, Pekka Roytta, Ahti Jaatinen-Värri. Performance and flow fields of a supersonic axial turbine at off-design conditions. Proceedings of the Institution of Mechanical Engineers Part A Journal of Power and Energy. 2023

[13] Deitch M.E. Technical gas dynamics. M.: Energy, 1974.

[14] Anderson, J. D. (1991). Fundamentals of aerodynamics. New York: McGraw-Hill.

[15] L. J. Pritchard, "An Eleven Parameter Axial Turbine Airfoil Geometry Model," in Gas Turbine Conference and Exhibit, Houst on, Texas, 1985.

[16] A Parametric Method of Turbine Blade Profile Design, J. Dunham, ASME 1974 International Gas Turbine Conference and Products Show, March 30–April 4, 1974

Zurich, Switzerland.

[17] M. E. Deich, Gas Dynamics of Turbomachinery Grids (Energoatomizdat, Moscow, 1996).

[18] E. M. Curtis, H. P. Hodson, M. R. Banieghbal, J. D. Denton, R. J. Howell, and N. W. Harvey, “Development of blade profiles for low-pressure turbine applications,” J. Turbomach. 119, 531–538 (1997).

[19] J. M. Anders, J. Haarmeyer, and H. Heukenkamp, “A parametric blade design system (Part I + II),” in Turbomachinery Blade Design Systems (Von Karman Inst. for Fluid Dynamics, Rhode Saint Genèse, Belgium, 1999), in Ser.: Von Karman Institute for Fluid Dynamics: Lecture Series 1999–2002.

[20] B. M. Aronov, M. I. Zhukovskii, V. A. Zhuravlev,

Profiling Aircraft Gas Turbine Blades (Mashinostroenie, Moscow, 1975)

[21] K. Siddappaji, M. G. Turner, and A. Merchant, “General capability of parametric 3d blade design tool for turbomachinery,” in Proc. ASME Turbo Expo 2012: Turbine Technical Conf. and Expo., Copenhagen, Denmark, June 11–15,2012 (ASME, New York, 2012), paper no. GT2012-69756, pp. 2331–2344.

[22] T. Korakianitis and G. I. Pantazopoulos, “Improved turbine-blade design techniques using 4th-order parametric-spline segments,” J. Comput.-Aided Des. 25, 289–299 .993).

[23] N. Kladovasilakis, T. Efstathiadis, I. Aslanidou, and A. Kalfas, “Rotor blade design of an axial turbine using non-ideal gases with low real-flow effects,” Energy Procedia 142, 1127–1132(2017)

[24] M. E. Deich, G. A. Fillipov, and L. Ya. Lazarev, Atlas of Axial Turbomachinery Grid Profiles (Mashinostroenie, Moscow, 1965)

[25] M. Dejch and B. Trojanovskij, Untersuchung und Berechnung axialer Turbinenstufen, Berlin: VEB Verlag Technik, 1973.

[26] L.H. Back, R.F. Cuffel. Flow coefficients for supersonic nozzles with comparatively small curvature radius throats. AIAA conference, Vol.8, #2, 1970

[27] Tang, S. P., “Theoretical Dependence of the Discharge Coefficients of Axisymmetric Nozzles under Critical Flows,” Technical Report PR-118-PU, Department of Mechanical Engineering, Princeton Univ., 1969.

[28] R. L. Thornock. E. F. Brown. An Experimental Study of Compressible Flow Through Convergent-Conical Nozzles, Including a Comparison With Theoretical Results. ASME, Fluids Engineering Division, June 23, 1971. Re No. 71-WA/FE-3.

[29] John C. Kayser, Robert L. Shambaugh. Discharge coefficients for compressible flow through small-diameter orifices and convergent nozzles. Chemical Engineering Science, Vol. 46, No. 7, pp. 1697-1711, 1991

[30] Arnberg, B.T., Britton, C.L., and Seidl W. F., “Discharge Coefficient Correlations for Circular-Arc Venturi Flowmeters at Critical (Sonic) Flow,” ASME JournaZ of Fluids Engineering, June 1974

[31] Ishibashi, M., and Takamoto, M., ‘Very Accurate Analytical Calculation of the Discharge Coefficients of Critical Venturi Nozzles with Laminar Boundary Layer,” Proceedings of the FLUCOME, Hayama, Japan, Sept. l-4, 1997.

[32] A. N. Johnson, P. I. Espina, G. E. Mattingly, J. D. Wright and C. L. Merklet. Numerical characterization of the discharge coefficient in critical nozzles. National Institute of Standards and Technology. Workshop & Symposium, 1998

[33] ASME PTC 19.5-2004. Flow Measurement, Section 8 Sonic Flow Nozzles and Venturis — Critical Flow, Choked Flow Condition. Reaffirmed 2013.

[34] IS0 9300: 1990 (E)., ‘Measurement of Gas Flow by Means of Critical Flow Venturi Nozzles,” Geneva, Switz., 1990.

[35] Chao Wang, Peijuan Cao, Chunhui Li, Hongbin Ding, Lishui Cui. Influence of wall roughness on boundary layer transition position of the sonic nozzles. Measurement. Volume 139, June 2019, Pages 196-204

[36] AGARD ADVISORY REPORT 32. Sonic Nozzles for Mass Flow Measurement and Reference Nozzles for Thrust Verification. Report of the Fluid Dynamics Panel Working Group 19

[37] F. Vulovic, E. Vincendeau, J.P. Vallet, C. Windenberger O. Villanger, J. Bosi. Influence of thermodynamic calculations on the flow rate of sonic nozzles. 4th International Symposium on Fluid Flow Measurement Denver, Colorado USA June 27 - 30, 1999

[38] Vance F. Dippold. Computational Simulations of Convergent Nozzles for the AIAA 1st Propulsion Aerodynamics Workshop. NASA/TM—2014-218329, 2014

[39] N. M. Kuluva, G. A. Hosack. Supersonic Nozzle Discharge Coefficients at Low Reynolds Numbers. AIAA JOURNAL, VOL. 9, NO. 9, 1971

[40] Andrew J. Szaniszlo. experimental and analytical sonic nozzle discharge coefficients for Reynolds numbers up to 8x10^6. NASA TN D-7848, 1975

[41] A. Haddad, H. Kbab. Application of De-Laval Nozzle Transonic Flow Field Computation Approaches. International Journal of Mechanical, Aerospace, Industrial and Mechatronics Engineering Vol:7, No:2, 2013

[42] Lavrukhin G.N. Aero gas dynamics of jet nozzle. T. 1. Internal characteristics nozzle. M.: Science. FIZMATLIT, 2003. 376 p

[43] G. N. Abramovitch. Applied Gas Dynamics. Third Edition, 1973

[44] Rao G.V. Evaluation of conical nozzle thrust coefficient // ARS J.- 1959, #8.

[45] A. Mccabe, Ph.D. Design of a supersonic nozzle. The Mechanics of Fluids Department, University of Manchester. Reports and Memoranda No. 3440* March 1964.

[46] Asha, G. D. N. Mohana, K. S Priyanka, and D.

Govardhan., Design of Minimum Length Supersonic Nozzle using the Method of Characteristics, International Journal of Innovative Technology and Exploring Engineering 9, 2019.).

[47] Marta Zocca , Paolo Gajoni , Alberto Guardone. NIMOC: A design and analysis tool for supersonic nozzles under non-ideal compressible flow conditions. Journal of Computational and Applied Mathematics 429, 2023

48] Box, G. E. P., & Behnken, D. Some new three-level designs for the study of quantitative variables. Technometrics, 2, 455–475. -1960.

[49] Menter F.R., Langtry R., Kuntz M. Ten years of Industrial Experience with the SST turbulence model// Proceedings of the 4th International Symposium on Turbulence, Heat and Mass Transfer, Antalya, Turkey, 2003.

